

Studies on the Effect of Number of Sugar Moiety in the Antifreeze Activity of Homodimeric AFGPs

Mija Ahn, Ravichandran N. Murugan, Eunjung Kim,[†] Jun Hyuck Lee,^{†,#} Chaejoon Cheong, Shin Won Kang,[‡] Hee Jung Park, Song Yub Shin,[§] Hak Jun Kim,^{†,#,*} and Jeong Kyu Bang^{*}

Division of Magnetic Resonance, Korea Basic Science Institute, Ochang, Chung-Buk 363-883, Korea. *E-mail: bangjk@kbsi.re.kr

[†]Division of Polar Life Sciences, Korea Polar Research Institute, Incheon 406-840, Korea. *E-mail: hjkim@kopri.re.kr

[‡]Department of Chemistry, Pusan National University, Pusan 609-735, Korea

[§]Department of Bio-Materials, Graduate School and Department of Cellular & Molecular Medicine, School of Medicine, Chosun University, Gwangju 501-759, Korea

[#]Department of Polar Sciences, University of Science and Technology, Incheon 406-840, Korea

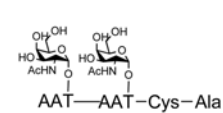
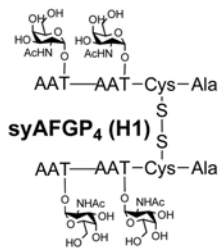
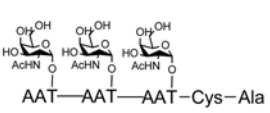
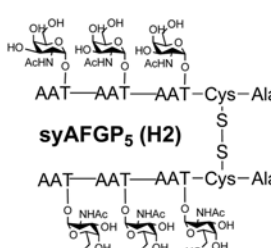
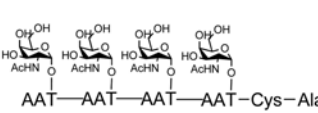
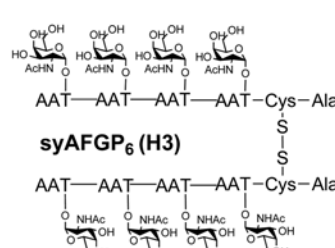
Received February 29, 2012, Accepted April 2, 2012

Key Words : Antifreeze glycoproteins (AFGPs), Thermal hysteresis activity, Ice morphology, Hexagonal bipyramid, Carbohydrate

Antifreeze glycoproteins (AFGPs) are found in the plasma of deep sea polar fish such as the Antarctic notothenioids and the northern cods.¹⁻⁴ The AFGPs consist of repeating tripeptide units, Alanyl-Alanyl-Threonyl (Ala-Ala-Thr)_{n=4-50} units, connected with the disaccharide β -D-galactosyl-(1 \rightarrow 3)- α -D-N-acetylgalactosamine through a glycosidic bond at the secondary hydroxyl group of the threonine residue.⁵ Eight distinct AFGP subtypes exist in nature. Among them, AFGP 1 is the largest weight (33.7 kDa) and AFGP 8 is the lowest molecular weight (2.6 kDa). AFGPs are able to depress the freezing temperature of the blood serum in fish enough to keep them from freezing in their sub-zero environment while the melting temperature remains unchanged. The gap between freezing point and melting point was referred to as thermal hysteresis (TH) and is taken as a primary manifestation of antifreeze activity by AFGPs.⁶ Within the hysteresis temperature gap, AFGPs modify the ice crystal habit, in that the AFGPs saturated ice crystal forms a unique shape, such as a hexagonal bipyramid. These effects prevent ice crystals from growing to a size where they would damage the fish's body.^{7,8} Despite AFGPs have been considered as a potent cryopreservation,⁹ obstacle to develop AFGPs as medicinal and industrial application is mainly due to the problem of understanding how AFGPs inhibit ice crystal growth. To obtain the antifreeze activity, the binding of AFGPs to the ice surface between the polar groups of the saccharide residue (the hydroxyl groups) and the ice surface are extremely important.¹⁰ AFGPs having two repeating units, (AAT*)_{n=2} AA which A is Ala, T* is threonine with disaccharide β -D-galactosyl-(1 \rightarrow 3)- α -D-N-acetylgalactosamine, does not show any detectable antifreeze activity whereas the three repeating units AFGP, (AAT*)_{n=3} AA displays antifreeze which is lower than the one having four repeating units.¹¹ These results implied that there is a definite relationship between the number of hydroxyl group of AFGPs and its antifreeze activity. Therefore, we focused on to study the dependence of the antifreeze

activity by increasing the number of hydroxyl group through the saccharide moiety which is linked by threonine residue. Considering our interest in the above relationship, herein for the first time we designed and evaluated the effect of homodimerization on AFGPs that eventually increases the number of sugar moieties on the antifreeze activity. Multivalency is known to increase the carbohydrate-protein interaction and has been exploited in the form of glycoclusters, glycopolymers and glycodendrimers.¹² We were intrigued by the possibility that the AFGPs with arms of different length, or with a different level of multivalency, might tune the antifreeze activity through binding more efficiently covering the higher surface area of the ice crystals. Based on the SAR studies, both the acetamide group (AcNH) on the sugar moiety and the methyl group of the threonine residue play a key role on the antifreeze activity.¹¹ However, the terminal galactose of disaccharide is not essential for the antifreeze activity. To simplify the synthesis, we have substituted the disaccharide β -D-galactosyl-(1 \rightarrow 3)- α -D-N-acetylgalactosamine with α -D-N-acetylgalactosamine in our AFGP analogues (Table 1). In the beginning, we attempted to synthesize the divergent AFGPs based on the rational scaffolding of L-lysine core structures on solid phase as previously explored in various glycodendrimers.¹³ But, we couldn't obtain the desired product due to the steric hindrance of highly dense sugar moiety during the synthesis. Therefore, in our revised strategy, dimeric AFGPs were successfully synthesized as pure oligomer by exploiting the disulfide bond formation. Disulfide bond formation is very attractive protocol because it is preparatively simple and easy access to the threonine linked homodimeric glycopeptides in good yield with high purity.¹⁴ Typically, AFGP 8 consists of (AAT*)_{n=4} AA which A is Ala, T* is threonine with O-linked α -D-N-acetylgalactosamine. For the synthesis of homodimeric AFGPs through disulfide bond formation, we chose the AFGP 8 which is the smallest subtype and easy to change the second Ala of the C-terminal with Cys. Scheme 1

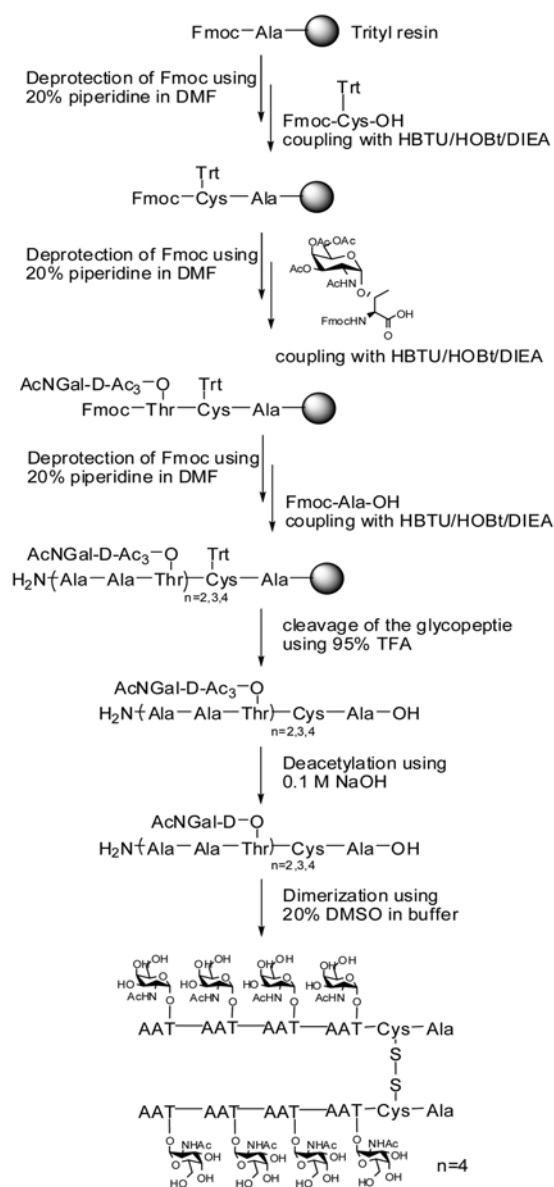
Table 1. Amino sequence of AFGP analogues examining TH activity and ice morphology

Structure	M.w	Structure	M.w
 <p>syAFGP₁ (L1)</p>	1107.3 [M+Na] ⁺	 <p>syAFGP₄ (H1)</p>	2189.9 [M+Na] ⁺
 <p>syAFGP₂ (L2)</p>	1554.4[M+Na] ⁺	 <p>syAFGP₅ (H2)</p>	3083.5 [M+Na] ⁺
 <p>syAFGP₃ (L3)</p>	2001.2[M+Na] ⁺	 <p>syAFGP₆ (H3)</p>	3974.9 [M+Na] ⁺

shows a protocol designed for the homodimeric AFGP synthesis by standard Fmoc-based solid phase. Under typical peptide synthesis, Fmoc-Cys(Trt)-OH was introduced into pre-loaded trityl resin after Fmoc group was removed using 20% piperidine in DMF. Then for glycosylated constructs,¹⁵ the glycosylated Fmoc-Thr(Ac₃- α -D-GalNAc) was coupled, using 3 equiv. of amino acid through the activation with HBTU (3 equiv.) and HOBt (3 equiv.) in the presence of *N,N*-diisopropylethylamine (3 equiv.) for 2 hours at room temperature, which was monitored by the Kaiser test. The remaining amino acids were introduced by standard Fmoc-chemistry.¹⁶ We repeated this procedure for the synthesis of remaining analogues of AFGPs having $n = 2, 3$ or 4. Finally, peptide cleavage/deprotection was accomplished with cleavage cocktail [trifluoroacetic acid-triisopropylsilane-water (TFA-TIS-H₂O; 95:2.5:2.5)] for 2.5 hours. Purification was accomplished *via* RP-HPLC, eluting with a gradient 10-90% acetonitrile in water, both containing 0.05% (vol/vol) trifluoroacetic acid (TFA). After purification, for deacetylation of sugar moieties, glycopeptides were then treated with 0.1 M NaOH in buffer stirred for 1 minute at room temperature, and the reaction was also monitored by RP-HPLC. Treatment of deacetylated AFGPs containing a single Cys residue using 20% DMSO in buffer as oxidants converted mono AFGP into the symmetrical homodimer AFGPs within 12 h at room temperature. After the completion of the disulfide bond formation, the solution was dilute to 2-fold and loaded directly to a preparative reverse-phase HPLC for purification

that gave 40-50% overall yield. The integrity of each purified homodimeric AFGPs was determined by MALDI-TOF-Mass spectrometry, and the observed molecular mass was found to agree with calculated values (Table 1).

Although the synthesis which rely on thiol-presenting subunits dimerization, is well known in dendrimers chemistry, disulfide-including the AFGP has never been exploited for the antifreeze activity. We considered that these divalent homodimeric AFGP architectures would provide new insights into the novel design of antifreeze analogues and the effect of increasing number of hydroxyl group through carbohydrate on the antifreeze activity. To determine the minimum number of tripeptide repeating units necessary for the antifreeze activity, AFGP (AAT^{*}) _{$n=2,3,4$} CA, [**L1** ($n=2$), **L2** ($n=3$), **L3** ($n=4$)] and the corresponding homodimeric AFGPs (**H1**, **H2** & **H3**) were produced through disulfide bond formation as shown in the Scheme 1. The antifreeze activity of each of **L1**, **L2**, **L3** and **H1**, **H2**, **H3** was evaluated by ice crystal morphology (Fig. 1) and TH activity (Fig. 2). **L1** exhibited neither hexagonal bipyramidal ice crystals nor thermal hysteresis activity. These results demonstrate that **L1** was not sufficiently large to control the ice crystal growth. Next, we added one more tripeptide unit, (AAT^{*}), into the **L1** to increase the number of hydroxyl group. As expected that the three-tripeptide **L2**, (AAT^{*}) _{$n=3$} CA, displayed both hexagonal bipyramidal ice crystal and thermal hysteresis activity. This indicated that **L2** has the optimum hydroxyl functional group to interact with water lattice to inhibit the ice crystal



growth. Interestingly, the activity of **L3**, which has four repeating units $(\text{AAT})_{n=4}\text{CA}$ was a little lower than that of **L2** even though Nishimura group reported¹⁰ that the thermal hysteresis activity of AFGPs has positive correlation with chain length. We subsequently hypothesized that the activity of **L2** might be the result of dramatic change in solution conformation due to presence of Cys which decides the orientation of carbohydrate moiety instead of Ala. The conformation of the AFGPs in the presence of ice has not been elucidated to date, but the creation of many hydrogen-bonds between the hydroxyls of the carbohydrate and the ice lattice surface remains to be the major hypothesis for its activity.¹⁷ Our convergent strategy by disulfide bond formation used in these initial studies provides divalent homodimeric AFGPs analogues that eventually double the interacting polar residues with the crystal lattice surface which might leads to the many fold increase in antifreeze activity. Antifreeze

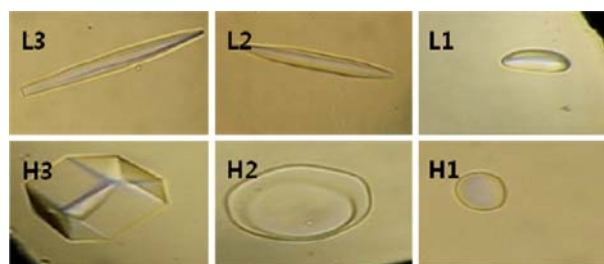


Figure 1. Ice-crystal morphologies in the presence of AFGP analogues.

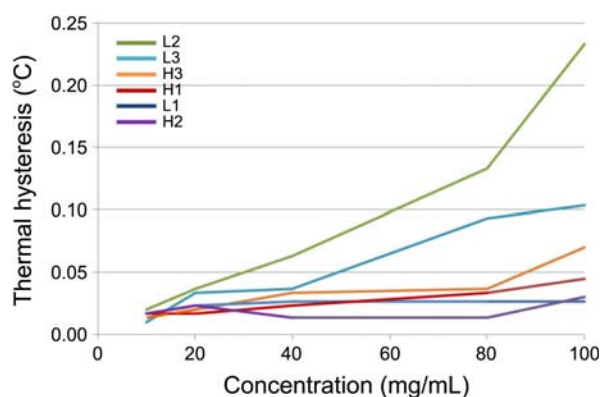


Figure 2. Thermal hysteresis activity of mono and homodimeric AFGPs.

activity for all the homodimers of AFGPs were evaluated by examining ice crystal morphology (Fig. 1) and thermal hysteresis activity (Fig. 2). Since **H1** is the homodimer of **L1** that didn't show any TH, we expected that the homodimerization of **L1** would lead to a strong binding AFGP analogue because it has the minimum number of sugar moieties necessary to induce the TH activity as in **L3**. But, unexpectedly, **H1** did not change the ice shape into hexagonal bipyramid and in addition it didn't show any detectable thermal hysteresis activity. From the above results, we concluded that the specific activity of **L3** compare to **H1** was derived from its intrinsic conformation. Next, the dimerization was carried out with the most active **L2** analogue from the above result to synthesize the **H2** and analyzed for the thermal hysteresis and ice morphology. However, the results of both TH activity and ice morphology change were not significantly different from those of the **H1**. Finally, **H3**, which has 8 tripeptide units, showed ice morphology as hexagonal type including the TH activity which is 3 times less than **L3**. From the evaluation of the activity discussed above, we also concluded that the conformation of the glycoprotein is also a key factor for antifreeze activity and the introduction of the disulfide bond formation destroys the active conformation of homodimeric AFGPs and interferes with the ability of the glycoprotein to prevent ice growth.

In summary, we obtained the homodimeric AFGP analogues as pure oligomers through the convergent disulfide bond formation. This strategy is very useful tool to increase the number of carbohydrate moieties of AFGP and needed to study further in order to lock the conformational flexibility.

Despite increase in the number of hydroxyl group which is essential to enhance the interaction with the ice crystal lattice, no antifreeze activity was detected for the homodimers. These results implied that the antifreeze activity depends not only on the number of carbohydrate moiety but also on the intrinsic conformations of each analogue. We expect that our contribution would provide new insights into the design of novel antifreeze analogues.

Experimental Section

Peptide Synthesis and Purification. Resin loaded with Fmoc-Ala-substituted Wang resin (0.51 mmol/g) was used as the support. The coupling of Fmoc-amino acids was performed with an equimolar mixture of *O*-Benzotriazole-*N,N,N',N'*-tetramethyl-uronium-hexafluorophosphate (HBTU), 1-hydroxybenzotriazole (HOBT) and *N,N*-diisopropylethylamine (DIEA) as the coupling reagents. After coupling the last amino acid, the Fmoc-group was removed with 20% piperidine/DMF, and the protected side chains and peptide-resin were deprotected and cleaved with a mixture of TFA-based reagent [trifluoroacetic acid-triisopropylsilane-water (TFA-TIS-H₂O; 95:2.5:2.5)] for 2 h at room temperature, and then precipitated with diethyl ether, and dried in the vacuum. The crude peptides were dissolved in 10% acetic acid and purified by a reversed-phase high-performance liquid chromatography (RP-HPLC) on a preparative (15 μ m, 10 \times 250 mm) C₁₈ Bondapak column using a water-acetonitrile gradient [30-70%/30 min] containing 0.05% trifluoroacetic acid (TFA).

Purity of the purified peptides was checked by a RP-HPLC on an analytical (10 μ m, 4.6 \times 150 mm) C₁₈ Vydac column using a water-acetonitrile gradient [30-70%/30 min] containing 0.05% trifluoroacetic acid (TFA).

For deacetylation of the carbohydrate protecting group, the peptides were dissolved in 0.1 M NaOH and shaken mixtures for 1 min at room temperature. After complete deprotection, the solution was neutralized with acetic acid and concentrated in vacuo. The peptides were purified by RP-HPLC and identified by MALDI-TOF-Mass analysis.

Mass spectrum (MALDI-TOF-Mass): L1, *m/z* 1107.3 [(M+Na)⁺, calcd 1107.8], L2, *m/z* 1554.4 [(M+Na)⁺, calcd 1554.2], L3, *m/z* 2001.2 [(M+Na)⁺, calcd 2000.7].

Disulfide Bond Formation. AFGP analogues L1, L2 and L3 (10 mg) was dissolved in water (10 mL). The pH of the solution was adjusted 8-9 by addition of ammonium bicarbonate. DMSO (2 mL) was added and the mixture was stirred at room temperature for 12 h. The progress of the oxidation reaction was checked by analytical C₁₈ RP HPLC column. At the completion of the reaction, usually 12 h, the solution was dilute 2-fold by the initial buffer (buffer A of HPLC) and loaded directly into a preparation C₁₈ RP HPLC column (Vydac, 7.5 \times 25 cm). MALDI-TOF MASS spectrometry was used to measure all synthetic AFGP analogues. The observed values agreed with the calculated values.

Mass spectrum (MALDI-TOF-Mass): H1, *m/z* 2189.9 [(M+Na)⁺, calcd 2189.5], H2, *m/z* 3083.5 [(M+Na)⁺, calcd

3083.9], H3, *m/z* 3974.9 [(M+Na)⁺, calcd 3974.6].

Antifreeze Activity. Antifreeze (thermal hysteresis) activity of synthesized AFGPs was measured using nanoliter osmometer (Otago Osmometers, Dunedin, New Zealand). The sample was placed on the surface of a temperature-controlled metal block and frozen rapidly at around -20 °C. The temperature was raised slowly until a single ice crystal remained. The temperature was lowered again slowly while the ice crystal morphology was maintained. The freezing point of the sample was taken by the temperature at which the rapid growth of ice crystal. The maximum difference between melting and freezing temperature was determined as the sample's TH value. The ice crystal morphology produced by AFGPs in distilled water and concentrations of the AFGP samples ranged from 0.0 to 100 mg/mL was examined and recorded under the microscope equipped with a Canon Digital Camera.

Acknowledgments. This study was supported by Korea Basic Science Institute's high field NMR research program grant T3022B (J.K.B) and National Agenda Project from The Korea Research Council of Fundamental Science & Technology (KRCF) and Korea Polar Research Institute (KOPRI) (Grant No. PG11010 and PE11100 to H.J.K).

References

- DeVries, A. L.; Wohlschlag, D. E. *Science* **1969**, *163*, 1073-1075.
- DeVries, A. L.; Komatsu, S. K.; Feeney, R. E. *J. Biol. Chem.* **1970**, *245*, 2901-2908.
- Komatsu, S. K.; DeVries, A. L.; Feeney, R. E. *J. Biol. Chem.* **1970**, *245*, 2909-2913.
- Feeney, R. E.; Yeh, Y. *Adv. Protein Chem.* **1978**, *32*, 191-282.
- Vandenhede, J. R.; Ahmed, A. I.; Feeney, R. E. *J. Biol. Chem.* **1972**, *247*, 7885-7889.
- Lie, S.; Wang, W.; Moos, E.; Jackman, J.; Mealing, G.; Monette, R.; Ben, R. N. *Biomacromolecules* **2007**, *8*, 1456-1462.
- Wu, Y.; Fletcher, G. L. *Biochem. Biophys. Acta Gen. Subj.* **2000**, *1524*, 11-16.
- Inglis, S. R.; Turner, J. J.; Harding, M. M. *Curr. Protein Pept. Sci.* **2006**, *7*, 509-522.
- Chaytor, J.; Ben, R. N. *Bioorg. Med. Chem. Lett.* **2010**, *20*, 5251-5254.
- Wierzbicki, A.; Taylor, M. S.; Knigh, C. A.; Madura, J. D.; Harrington, J. P.; Sikes, C. S. *Biophys. J.* **1996**, *71*, 8-18.
- Tachibana, Y.; Fletcher, G. L.; Fujitani, N.; Tsuda, S.; Monda, K.; Nishimura, S. I. *Angew. Chem. Int. Ed.* **2004**, *43*, 856-862.
- Johansson, E. M. V.; Crusz, S. A.; Kolomiets, E.; Buts, L.; Kadam, R. U.; Cacciarini, M.; Bartels, K.-M.; Diggle, S. P.; Ca'Mara, M.; Williams, P.; Loris, R.; Nativi, C.; Rosenau, F.; Jaeger, K.-E.; Darbre, T.; Reymond, J.-L. *Chem. Biol.* **2008**, *15*, 1249-1257 and references therein.
- Roy, R.; Zanini, D.; Meunier, S. J.; Romanowska, A. *J. Chem. Soc. Chem. Commun.* **1993**, 1869-1872.
- Euzen, R.; Reymond, J.-L. *Bioorg. Med. Chem.* **2011**, *19*, 2879-2887.
- Ahn, M.; Sohn, H.; Nan, Y. H.; Murugan, R. N.; Cheong, C.; Ryu, E. K.; Kim, E. H.; Kang, S. W.; Shin, S. Y.; Bang, J. K. *Bull. Korean Chem. Soc.* **2011**, *32*, 3327-3332.
- Bang, J. K.; Naka, H.; Teruya, K.; Aimoto, S.; Konno, H.; Nosaka, K.; Tatsumi, T.; Akaji, K. *J. Org. Chem.* **2005**, *70*, 10596-10599.
- Ebbinghaus, S.; Meister, K.; Born, B.; DeVries, A. L.; Gruebele, M.; Havenith, M. *J. Am. Chem. Soc.* **2010**, *132*, 12210-12211.